Experimental study of wave overtopping at rubble mound seawalls

Koosheh, Ali; Etemad-Shahidi, Amir; Cartwright, Nick; Tomlinson, Rodger; van Gent, Marcel R.A.

DOI
10.1016/j.coastaleng.2021.104062

Publication date
2022

Document Version
Final published version

Published in
Coastal Engineering

Citation (APA)
Koosheh, A., Etemad-Shahidi, A., Cartwright, N., Tomlinson, R., & van Gent, M. R. A. (2022). Experimental study of wave overtopping at rubble mound seawalls. *Coastal Engineering*, *172*, 1-11. Article 104062. https://doi.org/10.1016/j.coastaleng.2021.104062

Coastal Engineering 172 (2022) 104062

Contents lists available at ScienceDirect

Coastal Engineering

journal homepage: www.elsevier.com/locate/coastaleng

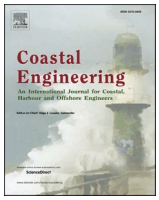

Experimental study of wave overtopping at rubble mound seawalls

Ali Koosheh [a], Amir Etemad-Shahidi [a,b,*], Nick Cartwright [a], Rodger Tomlinson [c], Marcel R. A. van Gent [d,e]

[a] School of Engineering and Built Environment, Griffith University, Southport, QLD, 4222, Australia
[b] School of Engineering, Edith Cowan University, WA, 6027, Australia
[c] Coastal and Marine Research Centre, Griffith University, Southport, QLD, 4222, Australia
[d] Department of Coastal Structures & Waves, Deltares, 2600, MH, Delft, the Netherlands
[e] Department of Hydraulic Engineering, TU Delft, 2628, CN, Delft, the Netherlands

ARTICLE INFO

Keywords:
Wave overtopping
Rubble mound seawall
Coastal structures
Laboratory experiment
Mean overtopping formula

ABSTRACT

Seawalls play a significant role in protecting coastal areas against wave attack and flooding. The accurate estimation of wave overtopping at seawalls is therefore crucial to adequately protect people and infrastructure in these regions. In this study, the mean wave overtopping rate at rubble mound seawalls was investigated through 140 small-scale physical model tests which adds to the limited existing data for this structure type in the extended CLASH database called EurOtop (2018). The combined dataset is used to evaluate the prediction skill of existing empirical formulae and to identify their limitations. The role of wave steepness on the mean overtopping rate is closely examined as it has not yet been considered properly in the EurOtop (2018) formulation. A new formula was derived using dimensional analysis and physical justifications of the overtopping phenomenon. The formula was found to provide a 40% decrease in *RMSE* in comparison to that of the EurOtop (2018). In addition, the new formula yields a BIAS ≈0, a significant improvement compared to −0.38 (non-dimensional discharge) of the EurOtop (2018) formula. The proposed formula has a simple form where non-dimensional overtopping discharge depends only on the relative crest freeboard and wave steepness, which were found to be the most important variables based on a sensitivity analysis.

1. Introduction

Based on recent observations and modelling, more severe storms and the high risk of flooding are expected for coastal areas due to climate change in the future. In order to mitigate this issue and protect the areas of human habitation and properties, effective coastal defence structures are needed. Seawalls are one such coastal defence system, are usually built parallel to shorelines with a variety of materials and geometries. Rubble mound seawalls are more common as they are easy to build and can dissipate wave energy effectively. They consist of armour layer(s) with natural quarry rock or prefabricated concrete blocks (e. g. cubes, tetrapods), a filter layer, and an impermeable core beneath. One of the important aspects of the design of a seawall is the determination of the required crest level to reduce overtopping risk as excessive wave overtopping can cause failures of the structure, financial losses (Neves et al., 2008) as well as threaten the safety of people and properties on the crest or the lee side. The mean overtopping rate (q) is commonly used for the design and assessment of coastal structures as it quantifies overtopping within a storm duration. To ensure the safety of the design, the mean overtopping rate should not exceed the allowable values specified in manuals (e. g. CEM, 2002; EurOtop, 2018).

Several approaches have been reported for the prediction of the mean wave overtopping rate which can be classified into numerical, physical, and data mining (e. g. EurOtop Neural Network) methods. Derived based on experimental datasets, empirical formulae are the most well-known and popular tools. These formulae are mostly derived through regression analysis in which dimensionless measured overtopping rates are correlated with dimensionless structural and hydraulic parameters using physical arguments. In practice, empirical formulae are preferred as they are more transparent in providing insight into the importance of different parameters as well as representing the physics of the overtopping process. The initial studies of wave overtopping at sloped seawalls are those of Goda (1971) and later by Owen (1980) in which a simple empirical formula was derived based on a limited number of effective parameters. Since then, several studies (e. g. van der Meer and Janssen, 1994; Besley, 1999) were carried out to extend the

* Corresponding author. School of Engineering and Built Environment, Griffith University, Southport, QLD, 4222, Australia.
E-mail address: a.etemadshahidi@griffith.edu.au (A. Etemad-Shahidi).

https://doi.org/10.1016/j.coastaleng.2021.104062
Received 24 August 2021; Received in revised form 5 November 2021; Accepted 26 November 2021
Available online 16 December 2021

knowledge and improve the existing empirical formulae. Within the CLASH European project, Steendam et al. (2004) gathered over 10,000 data from several measurements, and delivering important outputs such as a detailed evaluation of scale, model, and laboratory effects (De Rouck and Geeraerts, 2005; De Rouck et al., 2009). Using the CLASH database, Jafari and Etemad-Shahidi (2011) studied mean wave overtopping rate at simple sloped rubble mound structures and improved the prediction tools. A more recent formula for the prediction of mean wave overtopping rate at rubble mound structures has been developed by van der Meer and Bruce (2014) and released in EurOtop (2018) based on the extensive database from CLASH database and lately added data from different studies.

As mentioned before, the accurate prediction of the mean overtopping rate is crucial as its underestimation may cause extensive damage to infrastructures. On the other hand, the overestimation of the mean overtopping rate may result in high construction costs and loss of visual amenity due to the high crest level. In recent years, several studies have been devoted to improving formulae for structures such as inclined structures with a smooth impermeable surface (Etemad-Shahidi and Jafari, 2014; van Gent, 2020; Chen et al., 2020a,b), berm breakwaters (Pillai et al., 2017), single-layer cube armoured breakwaters (Vieira et al., 2021), smooth steep low-crested structures (Gallach-Sánchez et al., 2021) and rubble mound breakwaters with a crest wall (van Gent and van der Werf, 2019). For simple sloped rubble mound structures, large mean overtopping prediction errors were reported by Koosheh et al. (2020) when using the existing empirical formulae. They showed that EurOtop (2018) formula (Eq. 5), as the most recent one, results in very scattered predictions. Besides the complicated nature of the overtopping phenomenon and measurement errors, the appropriate use and scaling of effective wave and structural parameters could play a major role in the accuracy of analysis (Baldock et al., 2012). The reliability of an empirical formula depends on the quality and quantity of data (Pillai et al., 2017). Only, a limited number of overtopping records (120 data) for rubble mound seawalls are available in the literature. A significant portion of records belongs to the structures with slopes of $\tan\alpha = 0.5$ and milder, while limited data is reported for steeper slopes. It is then possible to improve the existing predictive tool for the mean overtopping rate at rubble mound seawalls by adding some data to cover the existing gaps in terms of key parameters as well as revising the formulation.

The present study aims to better understand wave overtopping at rubble mound seawalls through physical model tests. To achieve this aim, the existing limited data related to rubble mound seawalls was obtained, and the gaps in terms of key parameters were investigated. The experiments were designed to extend the available dataset and fill the identified gaps. Using the existing data (hereafter ETS) and those collected from the new 2D small-scale physical model tests (hereafter AK), a revised formula was proposed based on physical justifications and reasonings. This paper is organized as follows: Subsequent to the introduction, section 2 provides an overview of the most important empirical formulae for the prediction of mean wave overtopping rate at rubble mound seawalls. Then, the details of the existing database, used for the analysis, and the undertaken physical modelling are discussed in sections 3 and 4 respectively. The prediction performances of empirical formulae using the existing and collected datasets are investigated, and their limitations are highlighted in section 5. This section also provides the details of the derivation of an enhanced formula along with the discussion of results. Finally, section 6 summarizes the findings and results of the study.

2. Background

Due to the stochastic nature of wave overtopping, it is difficult to describe this phenomenon in an exact deterministic way (EurOtop, 2018). The easiest way to assess the overtopping rate is using empirical formulae, which have been derived based on experimental data. Hence, their applications are restricted to the corresponding test conditions and structural geometry. As a simplified representation of the physics of the process, the empirical formulae relate dimensionless wave overtopping rate to the key parameters of the phenomenon using some factors to adjust the effects of the roughness of the structure's surface, the obliquity of wave direction, etc. Here, a brief overview of the most important empirical formulae for the prediction of the mean wave overtopping rate applicable to rubble mound seawalls is provided.

Owen (1980) proposed an exponential equation form for the prediction of mean overtopping rate at simple sloped impermeable structures:

$$\frac{q}{gH_{m0}T_m} = a\exp\left(-b\frac{R_c}{H_{m0}}\sqrt{\frac{s_{om}}{2\pi}}\frac{1}{\gamma_f}\right) \tag{1}$$

where T_m is the mean period of the incident waves, g is gravity acceleration, q is the mean overtopping discharge per unit of structure width, and s_{om} stands for wave steepness, defined as:

$$s_{om} = \frac{H_{m0}}{L_{om}} \tag{2}$$

The parameter H_{m0} represents the spectral wave height, and R_c is the crest freeboard. The roughness reduction factor (γ_f), makes it possible to generalize the formula to the structures with different roughness and material types. Here, a and b are empirical coefficients that depend on the seaward slope of the seawall. van der Meer and Janssen (1994), involved the effect of wave breaking conditions on overtopping formulation, and proposed below equations:

$$If\ Ir_{op} < 2;\quad \frac{q}{\sqrt{gH_{m0}^3}}\sqrt{\frac{s_{op}}{\tan\alpha}} = 0.06\,exp\left(-5.2\frac{R_c}{H_{m0}}\frac{\sqrt{s_{op}}}{\tan\alpha}\frac{1}{\gamma_f\gamma_h\gamma_\beta}\right) \tag{3}$$

$$If\ \ Ir_{op} > 2;\quad \frac{q}{\sqrt{gH_{m0}^3}} = 0.2\,exp\left(-2.6\frac{R_c}{H_{m0}}\frac{1}{\gamma_f\gamma_h\gamma_\beta}\right) \tag{4}$$

where Ir_{op} represents Iribarren number (breaker parameter) defined by $tan\,\alpha/\sqrt{s_{op}}$, α is the seaward slope of structure, and s_{op} is wave steepness defined by H_{m0}/L_{op}. The reduction factors of γ_β and γ_h, with the maximum value of one, account for the effects of wave obliquity and water depth at the toe of the structure. In Eq. (3), the wave period and slope of the structure have a large influence on the wave overtopping for plunging (breaking) waves.

For rubble mound structures at deep water conditions, since incident waves are mostly non-breaking, EurOtop, (2007) proposed Eq. (4) but without the effect of water depth (γ_h). Christensen et al. (2014) reported the EurOtop, (2007) formula significantly underestimates wave overtopping for the long waves. This formula has recently been updated by EurOtop (2018) based on a larger database and the wider ranges of parameters as:

$$\frac{q}{\sqrt{g\cdot H_{m0}^3}} = 0.09\quad \exp\left[-\left(1.5\frac{R_c}{H_{m0}\cdot\gamma_f\cdot\gamma_\beta}\right)^{1.3}\right] \tag{5}$$

This formula gives almost similar predictions of overtopping rates to those of TAW, (2002) and EurOtop, (2007). The main difference can be found for low crested structures ($R_c/H_{m0} < 0.5$) where EurOtop, (2007) formula is not validated (van der Meer and Bruce, 2014).

There is still some dispute over the optimal value of the roughness factor for different armour types (e. g. Medina and Molines, 2016; Eldrup and Lykke Andersen, 2018). For rock armoured structures with impermeable cores, EurOtop (2018) recommends the roughness factor $\gamma_f = 0.55$ (two layers) and 0.6 (one layer). These values are valid for $2.5 < Ir_{m-1,0} < 4.5$, while for $Ir_{m-1,0} > 5$, EurOtop (2018) proposes applying a modification to the roughness factor as given below:

$$\gamma_{fmod} = \gamma_f + \frac{(Ir_{m-1,0} - 5)(1 - \gamma_f)}{5} \quad (6)$$

Recently, for rock-armoured slopes with an impermeable core, Chen et al. (2020b) proposed that the roughness factor depends on the wave and geometrical conditions.

3. Existing database

EurOtop (2018) database is a large collection of wave overtopping measurements that have mostly been collected during the CLASH project (Steendam et al., 2004). This extended database includes over 18, 000 records on a variety of coastal structures for both laboratory and field measurements. For each record, there are 35 parameters describing the wave characteristics in deep water and at structure's toe, foreshore conditions, and structural geometries along with their corresponding mean overtopping rate (Zanuttigh et al., 2016) (See Fig. 1). Regarding wave parameters, the spectral wave height (H_{m0}) and period ($T_{m-1,0}$) at the toe of the structure are generally considered as the most important ones. Accordingly, the wave steepness at the structure's toe can be defined as $s_{m-1,0} = H_{m0}/ L_{m-1,0}$ where $L_{m-1,0} = (g/2\,\pi)\, T^2_{m-1,0}$. The key parameters to describe structural features are crest freeboard (R_c), and the seaward slope of structure ($tan\ \alpha$).

In the present study, following van Gent et al. (2007), several filters were applied to the existing database (extended CLASH database called EurOtop) to isolate data relevant to rubble mound seawalls. In the first step, very low overtopping rates ($q < 10^{-6}$ m^3/s/m) were excluded, which are likely to be affected by greater error measurements in small-scale tests. Then large-scale records with $H_{m0} > 0.5$ were excluded due to possible scale effects (Verhaeghe, 2005; Jafari and Etemad-Shahidi, 2011). The CLASH database (Steendam et al., 2004) characterizes each record by reliability and complexity factors, *RF* and *CF*, which vary from 1 to 4. Accordingly, $RF = 1$ means all parameters for the corresponding record were available/measured within the test procedure, hence, no secondary estimation or assumption based on available parameters was required. On the other hand, the records with $RF = 4$ are considered as the least reliable data which should not be used for analysis, following van Gent et al. (2007). Likewise, *CF* indicates how well the structural features are defined where $CF = 1$ is used for structures with simple geometry. Here, the records with the highest level of complexity ($CF = 4$) or the lowest reliability ($RF = 4$) were removed. Regarding the structural geometry, the records of simple (straight) sloped structures (without berm and $tan\ \alpha_u = tan\ \alpha_d$), with emerged crest ($R_c > 0$), and without crest wall ($R_c = A_c$) were selected for further analysis. Here, A_c is the crest height of armor unit, α_u and α_d are the upper and lower slopes of the structure. As the present study focuses on rubble mound seawalls that have an impermeable core, the records with roughness factors of $\gamma_f = 0.55$, 0.6 were selected. The application of mentioned filters to the existing database resulted in 120 records (ETS dataset), including 7 different references. More details about the ranges of parameters are shown in Table 1. It should be mentioned that all ETS data, belonging to the tests with head-on incident waves ($\beta = 0$), includes only 6 records of one-layer rock seawall ($\gamma_f = 0.6$), and all the other 114 data are seawalls with two layers of rock ($\gamma_f = 0.55$).

Table 1
Ranges of key parameters for ETS and AK datasets.

Parameter	ETS dataset	Present study (AK dataset) Scale: 1/50
R_c (m)	0.05–0.35	0.08–0.21
H_{m0} (m)	0.08–0.22	0.07–0.13
$T_{m-1,0}$ (s)	1.13–3.23	1.07–1.96
h_t (m)	0.15–0.75	0.35–0.48
q (m^3/s/m)	10^{-6} – 1.59×10^{-2}	1.23×10^{-6} – 1.35×10^{-3}
R_c/ H_{m0}	0.46–2.58	0.75–2.5
$tan\ \alpha$	0.25–0.75	0.5–0.66
$s_{m-1,0}$	0.008–0.077	0.014–0.056
$Ir_{m-1,0}$	1.51–7.25	2.17–5.38
h_t/ H_{m0}	1.37–7.00	3.20–6.66
$G_c/ L_{m-1,0}$	0–0.07	0
q^*	7.56×10^{-6}– 5.8×10^{-2}	1.24×10^{-5} – 1.04×10^{-2}
Number of data points	120	140

Moreover, the ETS dataset covers a wide range h_t/ H_{m0} from 1.37 to 7, where h_t is water depth at the toe.

Fig. 2 represents the frequency histograms of obtained ETS data (120 records) for some dimensionless key parameters. In the case of wave steepness, the majority of data belongs to $0.01 < s_{m\text{-}1,0} < 0.02$. The histogram shows that almost half of ETS data were recorded in deep water conditions ($3 < h_t/ H_{m0}$).

The most significant gap in the ETS data can be found for the seaward slope of the structure. For the slopes steeper than $tan\ \alpha = 0.5$ there is only a limited number of records belonging to $tan\ \alpha = 0.75$, while no data exist for the slope of $tan\ \alpha = 0.66$. The given chart of Iribarren number shows that the existing data for rubble mound seawalls (ETS) are mostly non-breaking wave type ($Ir_{m-1,0} > 1.8$).

4. Experimental methodology

To address the gap in data described above, new two-dimensional small-scale physical model tests were conducted in the wave flume of the hydraulics laboratory of Griffith University, Australia. This wave flume has a length of 22.5 *m*, a width of 0.5 *m*, and a depth of 0.8 *m* (Fig. 3). The flume is equipped with a piston-type wavemaker which is able to generate both regular and irregular waves. The wavemaker is equipped with a dynamic absorption system that absorbs the reflected waves from the structure. In this study, 1 000 irregular waves with the JONSWAP spectrum and a peak enhancement factor (γ) of 3.3 were used. Three capacitance wave gauges were placed at the toe of the structure to measure the free surface of the water and estimate the wave parameters. As proposed by Mansard and Funke (1980), the three probes method was used to separate the incident and reflected waves assuming the following spacings:

$$X_{12} = L_{0p}/10 \quad (7)$$

$$L_{0p}/6 < X_{13} < L_p/3;\ \begin{cases} X_{13} \neq L_{0p}/5 \\ X_{13} \neq 3L_{0p}/10 \end{cases} \quad (8)$$

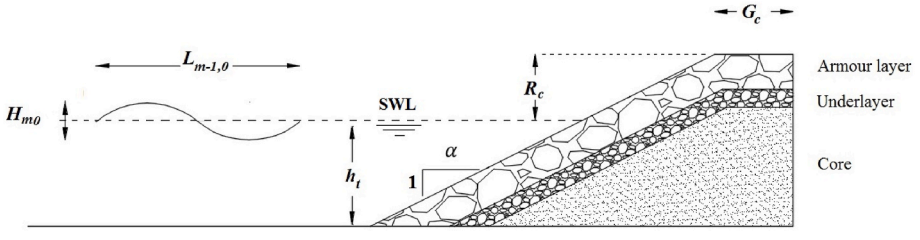

Fig. 1. Schematic diagram of rubble mound seawalls.

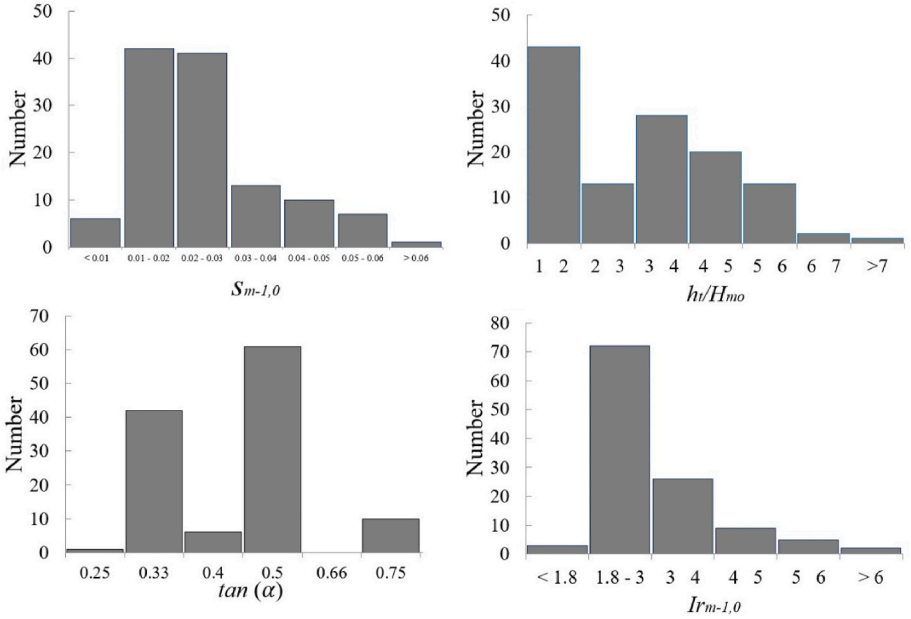

Fig. 2. The histogram of some key dimensionless parameters for the existing rubble mound seawall data (ETS) – (Total number of data points: 120).

where L_{0p} is the deep water wavelength obtained using peak wave period, X_{12} is the distance between the furthest probe to the structure and the middle one, and X_{13} represents the distance between the furthest probe and the nearest one to the structure (See Fig. 3). To reduce the influence of a reflective structure on the measured incident waves (evanescent wave model), the nearest probe (WG3) was placed far enough ($X_{3s} > 0.4\ L_{0p}$) from the toe (Klopman and van der Meer, 1999). Although, capacitance probes do tend to hold their calibration longer than other types (e. g. resistance-based), their calibrations were checked daily. In addition, the water surface level in the flume was regularly checked to avoid any possible effects of natural evaporation, facilities' leakages, and the overtopped volume of water. Tests were conducted on a rubble mound seawall with the crest height of 560 mm, the slopes of 1:1.5 and 1:2. The structure consists of an impermeable core made of plywood timber, underlayer with $D_{50} = 20$ mm, and armour layer with $D_{50} = 46$ mm. For both armour layer and underlayer, a minimum thickness of $2D_{50}$ was considered. To increase the friction between the rocks and timber's surface, a mixture of sand and water-proof glue was used on the slope of the seawall.

The impermeable crest (0.5 m long) of the seawall was covered by an acrylic sheet which was sealed at the flume's walls to prevent overtopped water leakage before reaching the collecting box. Overtopping measurement was achieved by using a small chute (66 mm width) on the rear side of the seawall's crest conducting the overtopped water in the box placed behind the structure. The chute, made of acrylic sheet, sitting on the collecting box's wall, was adjusted on the slope of 8%. Two capacitance wave gauges (WG4 and WG5), with initial submergence depths of 100 mm (Koosheh et al., 2021), were installed inside the overtopping box to read the water level. All signals received from mentioned probes were recorded at a frequency of 20 Hz using the National Instruments (NI) data acquisition card and home-developed MATLAB code. In addition, two high-speed cameras were installed to monitor the overtopping process during the experiment. One of the cameras was placed above the flume (top view), and another one recorded overtopping on the structure from the side view.

The tests programme was designed to fill the gap in the existing data for rubble mound seawalls (ETS) while covering the practical ranges of each parameter. A total number of 140 tests were conducted on the rubble mound seawall where half of the tests were carried out with a slope of 1:1.5, and the rest were the repetition of the same tests but with the slope of 1:2. With the water depth and peak wave period fixed, the significant wave heights were varied in the range of ± 20% of the design wave height (i. e. 0.08m, 0.09m, 0.1m, 0.11m, 0.12m). The details of collected data in the present study (AK dataset) are presented in Table 1. As seen, in terms of the ranges of some key parameters in both dimensional and dimensionless forms, AK data fall within the range of ETS data, however, identified gaps in terms of the slope of structure were filled. Significant wave heights and spectral wave periods varied between 0.07 and 0.13 *m* and 1.07–1.96 *s* respectively. The water depths between 0.35 and 0.48 *m* resulting in the relative crest freeboard of 0.75–2.5 were investigated in the present study. The range of Iribarren numbers ($Ir_{m-1,0} > 1.8$) shows that all tests were conducted with non-breaking wave conditions.

5. Results and discussion

5.1. Evaluation of existing empirical formulae

First, the performances of the existing empirical formulae for the prediction of dimensionless mean overtopping rate ($q^* = q/\sqrt{gH_{m0}^3}$) were evaluated. The performances of the Owen (1980) (Eq. 1) and EurOtop (2018) (Eq. 5) formulae, as the earliest and most recent ones, using all available data (ETS and AK), were visually compared in Fig. 4. Here, the solid line demonstrates the perfect agreement between measured and predicted values, and dashed lines are representative of 10 times over/underestimations. For both of the given formulae, about 72% of data lie within the mentioned ranges of the prediction. The predominant overestimation of Eq. (1) can be seen as a significant portion of data lie above the 10 times overestimation line. On the other hand, Eq. (5) shows underestimation, especially for the low rates of overtopping where more scatter in the data was observed.

Table 2 provides the accuracy metrics of the above-mentioned formulae (Eqs. 1 and 5). For a better comparison, the results are given for ETS and AK datasets, separately. Here, *BIAS* and Root Mean Square Error (*RMSE*) error metrics were used as below:

$$BIAS = \frac{1}{n}\sum_{i=1}^{n}\left[\log\left(q^*_{pred,i}\right) - \log\left(q^*_{mea,i}\right)\right] \quad (9)$$

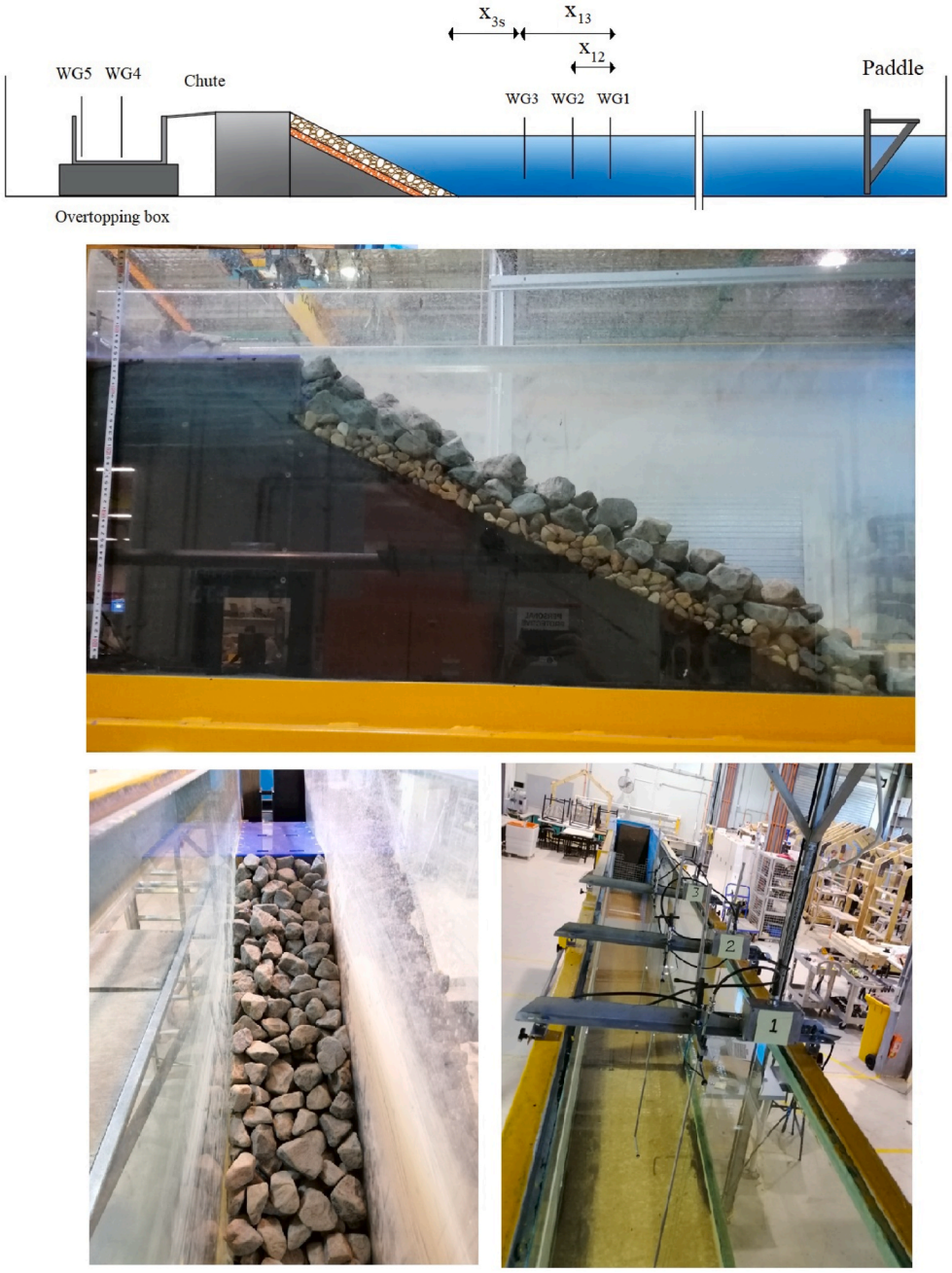

Fig. 3. Longitudinal cross-section of the flume of Griffith University (top); the picture of the constructed model (middle and bottom left); wave gauges (bottom right).

$$RMSE = \sqrt{\frac{1}{n}\sum_{i=1}^{n}\left\{\left[\log\left(q^{*}_{pred,i}\right) - \log\left(q^{*}_{mea,i}\right)\right]^{2}\right\}} \tag{10}$$

where n is the number of records, q^{*}_{pred} and q^{*}_{mea} are the predicted and measured mean overtopping rates, respectively. *BIAS* calculates the average of differences between measured and predicted values over the entire dataset. For a perfect prediction, *BIAS* is zero, while its positive and negative values show the overall over/under estimations. As *BIAS* by itself cannot represent a clear picture of scatter, *RMSE*, as a non-negative metric, is used for the better quantification of scatter. Accordingly, less *RMSE* means higher prediction accuracy while *RSME* = 0 stands for the perfect prediction.

As seen from Table 2, Eq. (1) with the overall *BIAS* = 0.71 (*BIAS* = 0.81 for ETS and *BIAS* = 0.62 for AK dataset) and *RMSE* = 0.94 significantly overestimates mean overtopping rate. However, this formula performs better for the AK data set rather than ETS one. Eq. (5) underestimates the mean overtopping rate with a *BIAS* value of −0.38 for all data, although, with *RMSE* = 0.86, it performs better than Eq. (1). For the AK dataset, Eq. (5) yields the *RMSE* of 0.73 which is less than that when applied to the ETS dataset.

The Discrepancy Ratio (*DR*) is another useful metric for performance evaluation. *DR* is defined as the ratio of the predicted value to the measured one where a good model should have its *DR* independent of the input parameter. If *DR* values for a model (formula) show dependency on a parameter, it implies that the relationship between the input and target parameters has been established improperly. Fig. 5 plots the *DR* values of Eq. (5) against some key dimensionless parameters. For both datasets (ETS and AK), an overall downward trend can be seen in panel (a). This trend is more remarkable for $R_c/\ H_{m0}\cdot\gamma_f > 3$, corresponding to the low overtopping rates, which means Eq. (5)

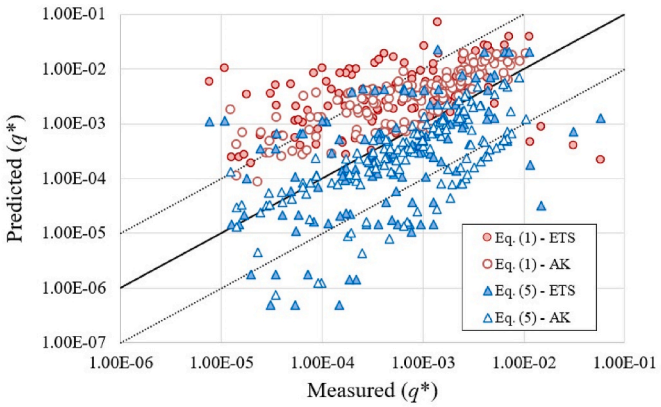

Fig. 4. Predicted vs measured mean wave overtopping rate at rubble mound seawalls using Eq. 1, Owen (1980) and Eq. 5, EurOtop (2018) formulae.

Table 2
Accuracy metrics of mean wave overtopping prediction using empirical formulae.

Dataset	Number of data	Eq. (5):EurOtop (2018)		Eq. (1):Owen (1980)	
		BIAS	RMSE	BIAS	RMSE
ETS	120	−0.29	0.98	0.81	1.13
AK	140	−0.45	0.73	0.62	0.74
All	260	−0.38	0.86	0.71	0.94

underestimates records with a high relative crest freeboard. On the other hand, in the case of $R_c/\ H_{m0}\cdot\gamma_f < 2$, representing the high values of overtopping, some overestimations are observed for ETS data although the prediction of AK data is less scattered and symmetric around the horizontal line ($DR = 1$).

Regarding the Iribarren number (panel b), when $Ir_{m-1,0} < 3.5$, the scatter of predicted data is more or less symmetric. However, for the higher values of this parameter ($Ir_{m-1,0} > 3.5$–4), Eq. (5) underestimates mean overtopping. Fig. 5 (c) displays DR values of predicted values against wave steepness ($s_{m\text{-}1,0}$). This plot is almost similar to that of the Iribarren number. For higher ranges of wave steepness ($s_{m\text{-}1,0} > 0.022$), less scatter can be seen without any particular trend. However, most of the data were underestimated in the range of $s_{m\text{-}1,0} < 0.022$ which shows that Eq. (5) has not been trained optimally for low steepness waves. To sum up, it seems Eq. (5) formula needs to be improved. This improvement could be achieved by enhancing the relationship between $R_c/\ H_{m0}\cdot\gamma_f$ and mean overtopping discharge (q^*), and more importantly by adding some other key parameters (e. g. wave steepness) to the prediction formulation.

5.2. Development of a new formula

To unify the whole dataset regardless of different model scales, analysis is usually carried out using dimensionless variables to relate influential wave and structural characteristics to the mean overtopping rate. The advantage of employing parameters in dimensionless form is to improve the analysis, fitting, and interpretation of results as well as the generalization of the formulation. Several parameters can contribute to wave overtopping at rubble mound seawalls, which can be found in the literature. Among all, the relative crest freeboard corrected with the roughness factor ($R_c/\ H_{m0}\cdot\gamma_f$), wave steepness ($s_{m\text{-}1,0}$), the seaward slope of the seawall ($tan\ \alpha$), and Iribarren number ($Ir_{m-1,0}$) have been used as the most effective ones.

For the derivation of the new formula, three factors namely simplicity, accuracy, and physical justification were considered. To achieve a simple formula, the less important parameters need to be identified and then eliminated. A sensitivity analysis was performed to investigate the importance of the mentioned parameters in which the effect of excluding each parameter on the accuracy was evaluated. Based on the initial regression analysis, the effects of the slope of the seawall and the Iribarren number on the mean overtopping rate were found to be marginal within the study range as their inclusion did not significantly improve the prediction accuracy. Accordingly, the relative crest freeboard and wave steepness were introduced as the dominant variables for the available dataset resulting in the form below:

$$q^* = \frac{q}{\sqrt{gH_{m0o}^3}} = f\left(\frac{R_c}{H_{m0}\cdot\gamma_f},\ s_{m-1,0}\right) \tag{11}$$

where the dimensionless mean overtopping rate in the form of $q/\sqrt{gH_{m0}^3}$

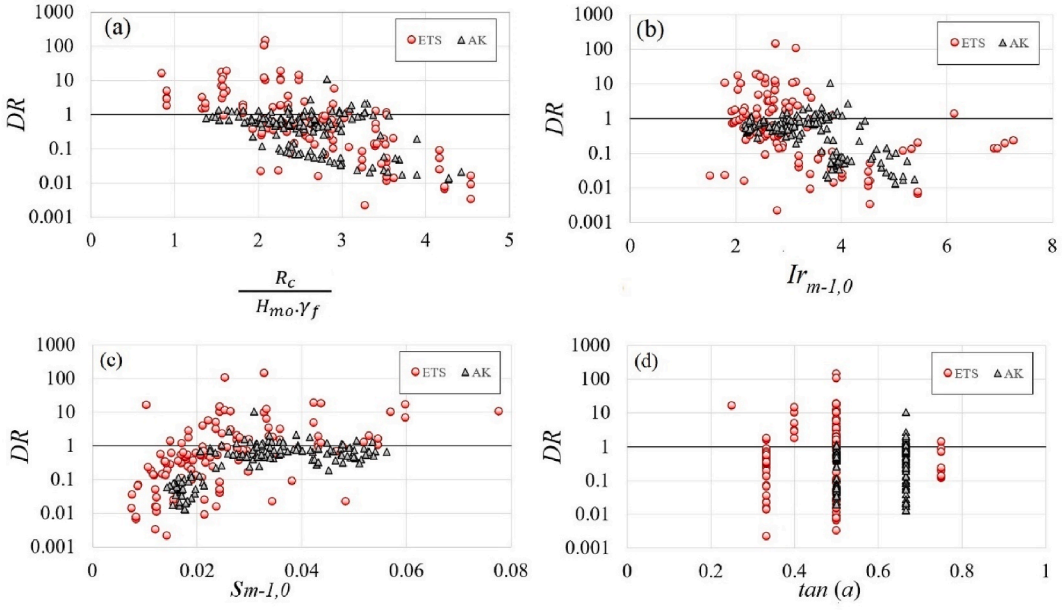

Fig. 5. Discrepancy ratios of predicted mean overtopping rate for EurOtop (2018) formula (Eq. 5) against (a): relative crest freeboard, (b): Iribarren number, (c): wave steepness, (d): seaward slope of the structure.

was selected as the target parameter. The elimination of the Iribarren number matches the recent finding of Ibrahim and Baldock (2020) that the breaker type is not a major factor in the scaling of the overtopping for non-breaking waves. However, this parameter is employed to assess wave run-up for breaking waves or shallow foreshores, having a secondary effect on the overtopping scaling.

To derive a formula for the prediction of mean overtopping rate, all available data (260 tests) including those collected within the present study (AK) and obtained from the existing database (ETS) were used. In this way, about two-thirds of records were randomly selected for training and the rest were used for validation (testing) of the model. Then, the extreme (minimum and maximum) values of train and test datasets were checked and swapped (if required) to ensure the test data ranges fall within the ranges of the train data in terms of dimensionless key parameters. The ranges of some key parameters for the train and test data are given in Table 3.

After investigating different functional forms between the governing parameters and the dimensionless mean overtopping rate (q^*), an exponential relationship was found the most appropriate one as given below:

$$q^* = a_1 \exp\left[a_2 \left(\frac{R_c}{H_{m0}\cdot\gamma_f}\right)^{a_3} \left(s_{m-1,0}\right)^{a_4}\right] \tag{12}$$

Here, to achieve the best fit to the data, the coefficients a_1, a_2, a_3 and a_4 need to be optimized. For this purpose, the Genetic Algorithm (GA) toolbox in MATLAB® was used to find the optimal values of the mentioned parameters. As an optimization tool, GAs belong to evolutionary algorithms which are inspired by biological processes. These kinds of algorithms are based on the survival principle of the fittest member in a population (series of solutions), which tries to retain genetic information from generation to generation (Roushangar and Koosheh, 2015). Here, *RMSE* was used as the fitness function which needs to be minimized in the optimization process. Besides the simplicity and accuracy of the formula, its physical justification should also be considered. Accordingly, a constrained optimization was performed based on previous studies and existing knowledge. The definition of constraints helps the algorithm to avoid inappropriate and physically unjustifiable values of optimized parameters even if they provide acceptable prediction accuracy. The two coefficients, a_1 and a_2, were constrained to be positive and negative, respectively to be physically justifiable and consistent with the general functional form presented in the literature. Considering the negative value of a_2, and knowing the fact that the relative crest freeboard ($R_c/ H_{m0}\cdot\gamma_f$) and wave steepness ($s_{m-1,0}$) have inverse relationships with the mean overtopping discharge, the coefficient a_3 and a_4 were forced to be positive. Finally, the following formula was obtained:

$$q^* = 0.034 \exp\left[-4.97\left(\frac{R_c}{H_{m0}\cdot\gamma_f}\right)^{1.12}\left(s_{m-1,0}\right)^{0.35}\right] \tag{13}$$

Fig. 6 represents the scatter plots of the measured vs predicted values by the proposed formula (Eq. 13) for the train and test datasets. Three inclined lines demonstrate conditions that the predicted rates are 10 times, equal, and 0.1 times of the measured rate. In comparison to Fig. 4, less scatter is observed as 94% of records lie between 10 times under/over estimation lines. The predicted values are almost symmetric around the perfect line for both sub-datasets. In addition, no significant difference can be seen between the scatter of train and test datasets as the test data were also well predicted by the proposed formula (Eq. 13).

Table 3
Ranges of key parameters for train and test datasets.

Parameter	Range	
	Train	Test
R_c/ H_{m0}	0.46–2.58	0.50–2.50
$tan\ \alpha$	0.25–0.75	0.33–0.75
$s_{m-1,0}$	0.008–0.077	0.008–0.052
$Ir_{m-1,0}$	1.51–7.25	1.79–6.89
h_t/ H_{m0}	1.37–7.00	1.44–6.66
q^*	7.56×10^{-6}– 5.8×10^{-2}	1.08×10^{-5}– 3.1×10^{-2}

The accuracy metrics of different formulae are shown in Table 4. It can be seen that the proposed formula with $RMSE = 0.51$ and $BIAS \approx 0$ outperforms other empirical formulae where about 40% improvement in prediction accuracy was observed compared to Eq. (5). Comparing the proposed formula (Eq. 13) with Eq. (1) demonstrates the superiority of the present formula with 45% less prediction errors. It is worth mentioning that 50% of test data (taken from ETS) is used for the derivation of Eq. (5), while the test dataset is fully unseen for the proposed formula (Eq. 13) of the present study.

In addition, Eq. (13) predicts AK data more accurately ($RMSE = 0.4$) than ETS data ($RMSE = 0.62$). The main reason for this could be the uniformity of AK data as it has been obtained from one set of experiments conducted by the authors. On the other hand, ETS data consists of several records which have been taken from different references of the existing database. This means that the ETS dataset includes different tests with different scales and measurement techniques, which could affect the results. For example, as some tests belonged to unknown references or the experiments date back three decades ago, it is not clear whether significant wave height ($H_s = H_{1/3}$) or spectral wave height (H_{m0}) has been measured, how the spectral wave period $T_{m-1,0}$ was obtained (not used for wave overtopping before 1999), and what wave spectrum was employed to generate incident waves.

Fig. 7 illustrates the scatter plots of *DR* values for the predicted mean overtopping rate by the proposed formula (Eq. 13) against some key dimensionless parameters. As expected, the AK dataset leads to less scatter and more accurate predictions rather than the ETS dataset. The comparison of panel (a) with that of Fig. 5 (Eq. 5), shows that an appropriate relationship has been established between relative crest freeboard and overtopping discharge in the newly proposed formula (Eq. 13). The scatter of data around $DR = 1$ is almost symmetric for the Iribarren number given in panel (b). The main improvement of the new formula can be seen in panel (c) where the large underestimation of low wave steepness by Eq. (5) has been compensated.

For practical design purposes, uncertainty and safety should be considered in the prediction formulation (Bruce et al., 2017; Shaeri and Etemad-Shahidi, 2021). This is commonly achieved through a safety margin included in the prediction formula based on the assigned level of risk. EurOtop (2018) assumes the coefficients of the formula as the stochastic variables, which are normally distributed. Hence, it describes the uncertainty by adding a multiple of the standard deviation ($N\ \sigma$) to

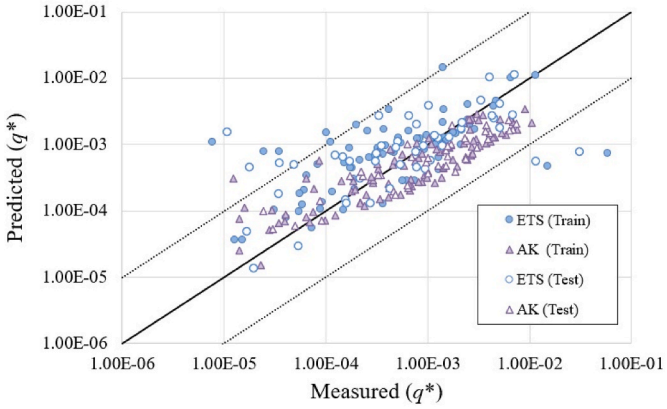

Fig. 6. Predicted vs measured mean wave overtopping rate at rubble mound seawalls using the newly proposed formula (Eq. 13) for train and test data (total records = 260).

Table 4
Comparison of the prediction performances of empirical formulae vs newly proposed one (Eq. 13).

Data	Eq. (5)		Eq. (1)		Eq. (13)	
	BIAS	RMSE	BIAS	RMSE	BIAS	RMSE
Train	−0.36	0.84	0.71	0.93	0.00	0.50
Test	−0.42	0.88	0.70	0.97	−0.01	0.53
ETS	−0.29	0.98	0.81	1.13	0.20	0.62
AK	−0.45	0.73	0.62	0.74	−0.17	0.4
All	−0.38	0.86	0.71	0.94	0.00	0.51

the coefficients. In the present study, following TAW (2002), one standard deviation of coefficients was added to obtain the design formula. This was achieved by (log) transforming the data to have a linear relationship between used parameters and mean overtopping discharge, and estimating the confidence intervals of the linear regression. The mean approach formula (Eq. 13), has a σ (0.034) = 0.016 and σ (4.97) = 0.45, hence the design formula can be expressed:

$$q^* = 0.05 \exp\left[-4.52\left(\frac{R_c}{H_{m0}\cdot\gamma_f}\right)^{1.12}\left(s_{m-1,0}\right)^{0.35}\right] \quad (14)$$

5.3. The new formula: features and physical justifications

The newly proposed formula (Eq. 13) for the prediction of mean wave overtopping rate at rubble mound seawalls follows the general functional form of the TAW (2002) and EurOtop, (2007); EurOtop, (2018) formulae. The power of $R_c/H_{m0}\cdot\gamma_f$ (1.12) implies a curve close to a line in a semi-logarithmic scale which is almost similar to that one obtained by Gallach-Sánchez et al. (2021) (=1.1). The most important change in the proposed formula is adding the effect of wave steepness as it has been overlooked in the EurOtop (2018) formula (Eq. 5) for non-breaking wave conditions. Wave steepness ($s_{m-1,0}$) raised to the power of 0.35 shows less sensitivity to this parameter in comparison to the relative crest freeboard, as expected. To some extent, this is similar to the proposed formula by Owen (1980) (Eq. 1) as well as van der Meer and Janssen (1994) formula (Eq. 3) for breaking wave conditions in which the mean overtopping rate has been related to the root square of the wave steepness ($s_{m-1,0}{}^{0.5}$). The results of the analysis, as given above, showed that adding wave steepness to the formulation can increase the prediction accuracy. Based on Eq. (13), for steeper waves (higher $s_{m-1,0}$), less overtopping discharge is expected than for waves with a lower steepness. Wave steepness is inversely proportional to the square of the wave period, and hence large wave periods lead to high overtopping. This can be explained as a longer wavelength (for the same wave height) will reach further leeward over the crest of a seawall than shorter wavelengths, thus resulting in more overtopping (Vieira et al., 2021).

To support the above-mentioned fact and investigate the effect of wave steepness variation on overtopping, the snapshots of three large waves taken from three tests with the same relative crest freeboard but different wave steepness are given in Fig. 8. Here, each column of the pictures shows the evolution of a particular single wave over the structure (wave steepness of 0.057, 0.035, and 0.018 for left, middle, and right columns, respectively). The pictures in each column have been taken with a few milliseconds delay. As seen in Fig. 8, for the wave steepness of $s_{m-1,0}$ = 0.057 (left column), the run-up flow is aerated at the front side (at $t = t_1$), while for the lower wave steepness ($s_{m-1,0}$ = 0.035 and 0.018), no air bubbles are observed. Looking at the third row (at $t = t_3$), in the left panel ($s_{m-1,0}$ = 0.057), the flow appears 'white' where only splashed water goes over the crest. The captured picture from the low wave steepness ($s_{m-1,0}$ = 0.018) in the third row (at $t = t_3$), shows wave overtopping in a rather smooth manner and profile as the wave surges over the crest. Finally, the comparison of the pictures given in the fourth row (at $t = t_4$) shows that the lower wave steepness, the thicker the overtopping layer on the crest, and hence the more overtopping volume. In conclusion, by reviewing the pictures given in Fig. 8, it is inferred that for the low values of wave steepness (say <0.022), overtopping flow shows different behaviour resulting in more overtopping discharge in comparison to that of high values of steepness.

6. Summary and conclusions

The present study was conducted to improve the existing predictive tools for the mean wave overtopping rate at rubble mound seawalls. For this purpose, a total number of 140 2D small-scale tests were conducted to extend the available limited dataset and cover the identified gaps in terms of some key parameters. The conducted tests cover the seaward

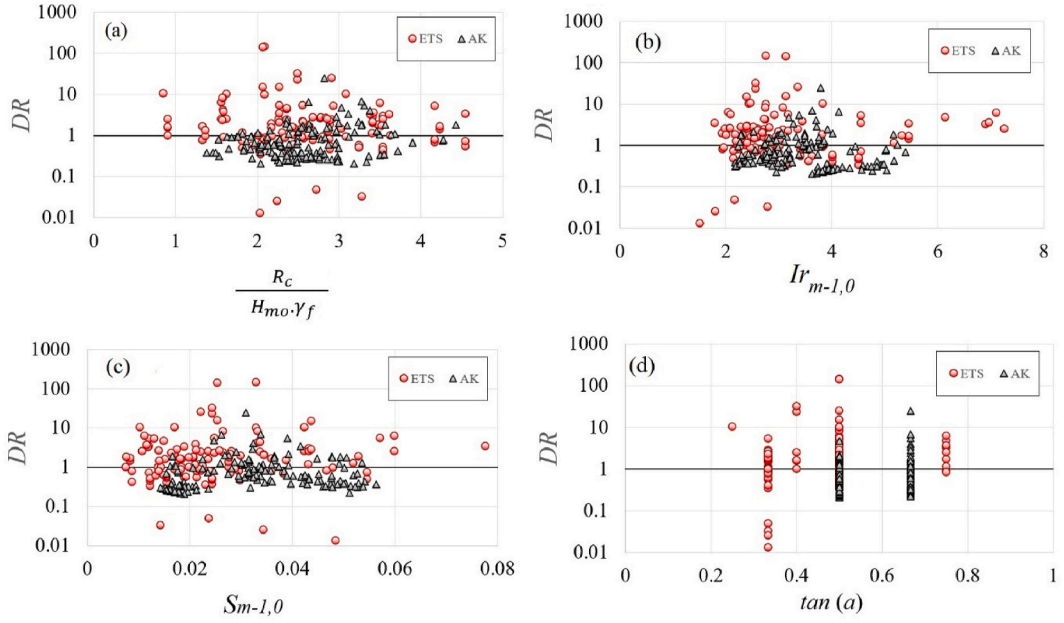

Fig. 7. Discrepancy ratios of predicted mean overtopping rate for newly proposed formula (Eq. 13) against (a): relative crest freeboard, (b): Iribarren number, (c): wave steepness, (d): seaward slope of structure.

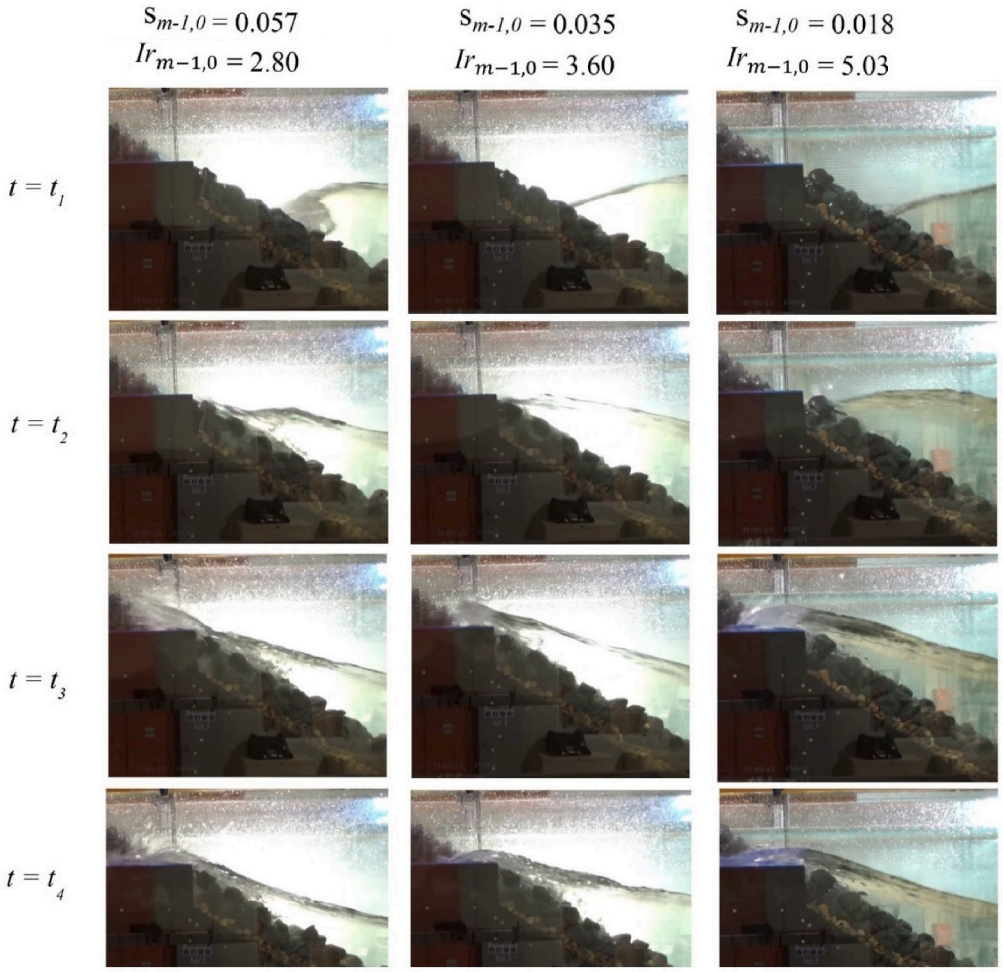

Fig. 8. Comparison of wave overtopping forms with different wave steepness (same wave height, crest freeboard but different wave periods). left row: $s_{m-1,0} = 0.057$, middle row: $s_{m-1,0} = 0.035$, right row: $s_{m-1,0} = 0.018$.

slopes of $tan\ \alpha = 0.5$ and 0.66, the wave steepness of $s_{m-1,0} = 0.014–0.056$, and the relative crest freeboard of $R_c/H_{m0} = 0.75–2.5$. The collected data from the present study (AK dataset) was added to 120 small-scale overtopping data of simple sloped rubble mound structures with impermeable cores, and without crown walls, taken from the extended CLASH (called EurOtop) database (ETS data).

The results of the analysis demonstrated the limitation of Eqs. (1) and (5) in the prediction of mean wave overtopping rate where more than 10 times errors were observed for about 28% of the used data. More detailed analysis on the performance of EurOtop (2018) formula (Eq. 5), as the most recent one, showed that it has not been trained optimally as data with low wave steepness ($s_{m-1,0} < 0.022$) were significantly underestimated. Moreover, for the high values of R_c/H_{m0}, Eq. (5) does not provide a good performance which shows some improvements need to be done in the formulation.

To derive a new improved formula, the available dataset was subdivided into train and test records. Conventionally known influential parameters of wave overtopping such as relative crest freeboard (R_c/H_{m0}), wave steepness ($s_{m-1,0}$), the seaward slope of structure ($tan\ \alpha$), and Iribarren number ($Ir_{m-1,0}$) were initially selected for the analysis. To obtain a compact formula, a sensitivity analysis was carried out. In this way, the mentioned parameters were excluded one by one, and the accuracies of the predicted formulae were investigated. The results of the sensitivity analysis highlighted the importance of relative crest freeboard and wave steepness for the studied case. As the effect of the structure slope on mean wave overtopping discharge was found to be negligible within the examined range of slopes, the structure slope was eliminated for further analysis. The exponential functional form was introduced as the best option to correlate the most important input parameters (R_c/H_{m0}, $s_{m-1,0}$) to the mean overtopping discharge (q^*).

A GA optimization tool was employed to find the optimal values of the coefficients of the selected functional form leading to the highest prediction accuracy. To avoid physically unjustifiable values of the coefficients, some constraints were imposed on the optimization algorithm. Finally, Eq. (13) was proposed which is similar to that of TAW (2002), EurOtop (2018), and Gallach-Sánchez et al. (2021) in terms of functional form, but considers the effect of wave steepness as well. Eq. (13) correlates the mean overtopping discharge to the relative crest freeboard raised to the power of 1.12 (close to a straight line on a semilogarithmic plot). In addition, wave steepness in the developed formula has a power of 0.35 (ignored in Eq. 5) which demonstrates the importance of wave period in the prediction of mean wave overtopping. Some snapshots of the conducted experiment were presented to demonstrate the effect of wave steepness on the overtopping form resulting in different overtopping volumes. The comparison of the waves with the same height but different periods (steepness), supporting the improved formula (Eq. 13), showed that for a lower wave steepness, the overtopping discharge increases.

The proposed formula (Eq. 13) is superior to Eqs. (1) and (5) as the improvement of 40% was observed in *RMSE* values in comparison to that of EurOtop (2018) formula (Eq. 5), and only 6% of the data was predicted with more than 10 times errors. With $BIAS \approx 0$, the

underestimation of Eq. (5), with BIAS = −0.38, as well as the overestimation of Eq. (1) (*BIAS* = 0.71) were improved. Moreover, the AK dataset was predicted 35% more accurately than the ETS dataset which could be due to the uniformity of the conducted test within the present study. The analysis of the Discrepancy Ratio (DR) against the key dimensionless parameters demonstrates the suitability of the proposed formula as the scatter of the plots is almost symmetric and no trend was detected. It is recommended to verify the observed dependency of wave overtopping on the wave steepness also for gentler (1:4 and milder) slopes (in combination with low steepness waves), than those examined in the present study.

Credit author statement

Ali Koosheh: Conceptualization, Methodology, Formal analysis, Investigation, Data curation, Writing - original draft, Visualization.

Amir Etemad-Shahidi: Conceptualization, Methodology, Analysis, Supervision, Writing, Review & Editing.

Nick Cartwright: Conceptualization, Supervision, Review & Editing

Rodger Tomlinson: Conceptualization, Supervision, Review & Editing

Marcel R. A. van Gent: Conceptualization, Supervision, Review & Editing

Declaration of competing interest

The authors declare that they have no known competing financial interests or personal relationships that could have appeared to influence the work reported in this paper.

Acknowledgments

The authors would like to acknowledge the financial support from Griffith University. The first author was funded by GUPRS and GUIPRS scholarships.

Glossary and Acronyms

A_c	Crest height
CF	Complexity factor
G_c	Crest Width
g	Gravity acceleration
H_{m0}	Spectral wave height
H_s	Average height of the 1/3 highest waves
h_t	Water depth at the structure's toe
$Ir_{m-1,0}$	Iribarren number defined as $tan\ \alpha / \sqrt{s_{m-1,0}}$
Ir_{op}	Iribarren number defined as $tan\ \alpha / \sqrt{s_{op}}$
L_{om}	Wavelength defined by $\frac{g}{2\pi}T_m{}^2$
$L_{m-1,0}$	Wavelength defined by $\frac{g}{2\pi}T_{m-1,0}^2$
L_{op}	Wavelength defined by $\frac{g}{2\pi}T_p{}^2$
q	Mean overtopping discharge per metre of structure width
q^*	Dimensionless mean overtopping discharge ($= q/\sqrt{gH_{m0}^3}$)
R_c	Crest freeboard
s_{om}	Wave steepness defined by $\frac{2\pi H_{m0}}{gT_m{}^2}$
s_{op}	Wave steepness defined by $\frac{2\pi H_{m0}}{gT_p{}^2}$
$s_{m-1,0}$	Wave steepness defined by $\frac{2\pi H_{m0}}{gT_{m-1,0}^2}$
T_m	Mean wave period (time domain)
$T_{m-1,0}$	Spectral wave period
T_p	Peak wave period
RF	Reliability factor
α	Seaward slope of structure
β	Wave obliquity
γ_β	Oblique wave factor
γ_f	Roughness factor
γ_{fmod}	Modified roughness factor
γ_h	Water depth factor
ETS	Rubble mound seawalls records taken form the extended CLASH database (EurOtop)
AK	Data collected within the present study

References

Baldock, T.E., Peiris, D., Hogg, A.J., 2012. Overtopping of solitary waves and solitary bores on a plane beach. Proc. R. Soc. A Math. Phys. Eng. Sci. 468, 3494–3516.

Besley, P., 1999. Wave Overtopping of Seawalls, Design and Assessment Manual. R&D technical report W178D, HR Wallingford.

Bruce, T., van der Meer, J.W., Pullen, T., Allsop, W., 2017. Wave overtopping at vertical and steep structures. Handb. Coast. Ocean Eng. Expand. Ed. 1 (–2), 633–661. https://doi.org/10.1142/9789813204027_0023.

Chen, W., Marconi, A., van Gent, M.R.A., Warmink, J.J., Hulscher, S.J.M.H., 2020a. Experimental study on the influence of berms and roughness on wave overtopping at rock-armoured dikes. J. Mar. Sci. Eng. 8, 446.

Chen, W., van Gent, M.R.A., Warmink, J.J., Hulscher, S., 2020b. The influence of a berm and roughness on the wave overtopping at dikes. Coast. Eng. 156, 103613.

Christensen, N.F., Thomsen, J.B., Andersen, T.L., Burcharth, H.F., 2014. Overtopping on rubble mound breakwaters for low steepness waves in deep and depth limited conditions. Coast. Eng. Proc. 6.

De Rouck, J., Geeraerts, J., 2005. CLASH-final report: full scientific and technical report. www.clash-eu.org.

De Rouck, J., Verhaeghe, H., Geeraerts, J., 2009. Crest level assessment of coastal structures—general overview. Coast. Eng. 56, 99–107.
Eldrup, M.R., Lykke Andersen, T., 2018. Recalibration of overtopping roughness factors of different armour types. In: Coasts, Marine Structures and Breakwaters 2017: Realising the Potential. ICE Publishing, pp. 1011–1020.
Etemad-Shahidi, A., Jafari, E., 2014. New formulae for prediction of wave overtopping at inclined structures with smooth impermeable surface. Ocean Eng. 84, 124–132. https://doi.org/10.1016/j.oceaneng.2014.04.011.
EurOtop, 2007. In: Pullen, T., Bruce, T., van der Meer, NL JW, Schüttrumpf, H., Kortenhaus, A. (Eds.), Wave Overtopping of Sea Defences and Related Structures-Assessment Manual. UK NWH Allsop. www. overtopping-manual. com.
EurOtop, 2018. In: van der Meer, J.W., Allsop, N.W.H., Bruce, T., De Rouck, J., Kortenhaus, A., Pullen, T., Schüttrumpf, H., Troch, P., Zanuttigh (Eds.), B., Manual on Wave Overtopping of Sea Defences and Related Structures. www.overtopping-manual.com.
Gallach-Sánchez, D., Troch, P., Kortenhaus, A., 2021. A new average wave overtopping prediction formula with improved accuracy for smooth steep low-crested structures. Coast. Eng. 163, 103800.
Goda, Y., 1971. Expected rate of irregular wave overtopping of seawalls. Coast. Eng. Japan 14, 43–51.
Ibrahim, M.S.I., Baldock, T.E., 2020. Swash overtopping on plane beaches-Reconciling empirical and theoretical scaling laws using the volume flux. Coast. Eng. 157, 103668.
Jafari, E., Etemad-Shahidi, A., 2011. Derivation of a new model for prediction of wave overtopping at rubble mound structures. J. Waterw. Port, Coast. Ocean Eng. 138, 42–52. https://doi.org/10.1061/(ASCE)WW.1943-5460.0000099.
Klopman, G., van der Meer, J.W., 1999. Random wave measurements in front of reflective structures. J. Waterw. Port, Coast. Ocean Eng. 125, 39–45.
Koosheh, A., Etemad-Shahidi, A., Cartwright, N., Tomlinson, R., Hosseinzadeh, S., 2020. The comparison of empirical formulae for the prediction of mean wave overtopping rate at armored sloped structures. Coast. Eng. Proc. 22.
Koosheh, A., Etemad-Shahidi, A., Cartwright, N., Tomlinson, R., van Gent, M.R.A., 2021. Individual wave overtopping at coastal structures: a critical review and the existing challenges. Appl. Ocean Res. 106, 102476.
Mansard, E.P.D., Funke, E.R., 1980. The measurement of incident and reflected spectra using a least squares method. Coast Eng. 154–172, 1980.
Medina, J.R., Molines, J., 2016. Roughness factor in overtopping estimation. Coast. Eng. Proc. 7.
Neves, M.G., Reis, M.T., Losada, I.J., Hu, K., 2008. Wave overtopping of Póvoa de Varzim breakwater: physical and numerical simulations. J. Waterw. Port, Coast. Ocean Eng. 134, 226–236.
Owen, M.W., 1980. Design of Seawalls Allowing for Wave Overtopping (Report No. Ex 924). Hydraul. Res. HR Wallingford.
Pillai, K., Etemad-Shahidi, A., Lemckert, C., 2017. Wave overtopping at berm breakwaters: experimental study and development of prediction formula. Coast. Eng. 130, 85–102.
Roushangar, K., Koosheh, A., 2015. Evaluation of GA-SVR method for modeling bed load transport in gravel-bed rivers. J. Hydrol. 527, 1142–1152.
Shaeri, S., Etemad-Shahidi, A., 2021. Wave overtopping at vertical and battered smooth impermeable structures. Coast. Eng. 166, 103889.
Steendam, G.J., van der Meer, J.W., Verhaeghe, H., Besley, P., Franco, L., van Gent, M.R.A., 2004. The international database on wave overtopping. In: Proc. 29th ICCE, vol. 4. World Scientific, pp. 4301–4313, 4301–4313.
TAW, 2002. Technical report wave run-up and wave overtopping at dikes. Tech. Advis. Comm. Flood Defence 42. Delft, Netherlands.
US Army Corps of Engineers, 2002. Coastal engineering manual. Eng. Manag. J. 1110, 2-1100.
van der Meer, J.W., Bruce, T., 2014. New physical insights and design formulas on wave overtopping at sloping and vertical structures. J. Waterw. Port, Coast. Ocean Eng. 140, 1–18. https://doi.org/10.1061/(ASCE)WW.1943-5460.0000221.
van der Meer, J.W., Janssen, J., 1994. Wave Run-Up and Wave Overtopping at Dikes and Revetments. Delft Hydraulics, publication no. 485. VdM VML EB MT2.
van Gent, M.R.A., 2020. Influence of oblique wave attack on wave overtopping at smooth and rough dikes with a berm. Coast. Eng. 160, 103734.
van Gent, M.R.A., van den Boogaard, H.F.P., Pozueta, B., Medina, J.R., 2007. Neural network modelling of wave overtopping at coastal structures. Coast. Eng. 54, 586–593.
van Gent, M.R.A., van der Werf, I.M., 2019. Influence of oblique wave attack on wave overtopping and forces on rubble mound breakwater crest walls. Coast. Eng. 151, 78–96. https://doi.org/10.1016/j.coastaleng.2019.04.001.
Verhaeghe, H., 2005. Neural Network Prediction of Wave Overtopping at Coastal Structures PhD Thesis. Gent university, Gent, BE.
Vieira, F., Taveira-Pinto, F., Rosa-Santos, P., 2021. New developments in assessment of wave overtopping on single-layer cube armoured breakwaters based on laboratory experiments. Coast. Eng. 166, 103883.
Zanuttigh, B., Formentin, S.M., van der Meer, J.W., 2016. Prediction of extreme and tolerable wave overtopping discharges through an advanced neural network. Ocean Eng. 127, 7–22. https://doi.org/10.1016/j.oceaneng.2016.09.032.